Theoretical model for enrichment of CH_3F nuclear-spin isomers by resonant microwave radiation

O. I. Permyakova
Institute of Semiconductor Physics, Russian Academy of Sciences, 630090 Novosibirsk, Russia

E. Ilisca
Laboratoire de Physique Théorique de la Matière Condensée, Université Paris 7–Denis Diderot, 2, Place Jussieu, 75251 Paris Cedex 05, France

P. L. Chapovsky*
Institute of Automation and Electrometry, Russian Academy of Sciences, 630090 Novosibirsk, Russia
(Received 29 August 2002; published 24 March 2003)

A theoretical model of coherent control of nuclear-spin isomers by microwave radiation has been developed. The model accounts the *M* degeneracy of molecular states and molecular center-of-mass motion. The model has been applied to the $^{13}CH_3F$ molecules. Microwave radiation excites the para state ($J=11$, $K=1$) which is mixed by the nuclear-spin-spin interaction with the ortho state (9,3). Dependences of the isomer enrichment and conversion rates on the radiation frequency have been calculated. Both spectra consist of two resonances situated at the centers of nuclear-spin-allowed and -forbidden transitions of the molecule. Larger enrichment, up to 7%, can be produced by strong radiation resonant to the forbidden transition. The spin conversion rate can be increased by two orders of magnitude at this resonance.

DOI: 10.1103/PhysRevA.67.033406 PACS number(s): 33.80.Be, 32.80.Bx, 32.80.Qk

I. INTRODUCTION

Nuclear-spin isomers of symmetrical molecules are fascinating objects [1]. Their properties are determined by the nuclear-spins deeply hidden in the molecule. Most known are the hydrogen isomers that demonstrate anomalous stability, one year at ambient temperature and pressure [2]. Latest results on hydrogen isomers can be found in Refs. [3,4], and references therein. Many other molecules have spin isomers too. But, so far their physical properties remain almost unknown. This makes investigations of spin isomers fundamentally important. Spin isomers have also practical applications, e.g., for isomer selective chemical reactions [5,6], or in isomer-enhanced NMR techniques [7,8]. These applications are developed solely with hydrogen isomers. Extension to other molecules requires efficient methods of isomer enrichment. For a long time enrichment of only hydrogen isomers was possible. Recently a few separation methods for polyatomic molecules have been developed (see the review [9]) that have advanced the field significantly. New enrichment methods are needed for further progress.

An alternative approach to the problem of isomer enrichment is based on the use of strong electromagnetic radiation. There are two modifications of the method. In the first one [10,11] (for an earlier discussion of the radiation effects see Ref. [12]), the radiation populates specific states of one spin isomer situated in the vicinity of the states of another isomer which consequently leads to enrichment. In the second method [13], enrichment appears due to the combined action of population transfer, dynamical shift of molecular levels, and light-induced coherence. The latter method (coherent control of spin isomers) promises to be more efficient. To avoid any confusion, we note that the light-induced enrichment resulting from stimulating conversion of spin species differs radically from the previously known separation methods, e.g., the light-induced-drift method spatially separates the isomers [9].

There is no proof yet that light-induced enrichment of spin isomers is feasible. We are aware of only one attempt to verify the proposals [14]. This involved microwave excitation of rotational transition in CH_3F. The experiment did not give a positive result. At the time when this experiment was performed, only a qualitative theoretical model of the light-induced enrichment was available [10]. Presently, the understanding of the underlying physics has been improved substantially. In view of further experiments in this area it is desirable to examine the microwave-induced enrichment of CH_3F spin isomers in more detail. This is the goal of the present paper. Existing theoretical models of coherent control cannot be directly used for a quantitative analysis because these do not account for the *M* degeneracy of molecular states. Accounting for such degeneracy is another goal of this paper.

II. QUALITATIVE PICTURE AND KINETIC EQUATION

Previous analysis has shown that significant enrichment can be obtained if radiation interacts with the states having large population differences. In this context, microwave excitation is not the best option; but it has some advantages also. Theoretical description is simpler for pure rotational excitation. The level positions are better known for the ground vibrational states. From the experimental side, it is easier to find a radiation having proper frequency because of better frequency tunability of microwave sources.

We start with a brief qualitative description of the phenomenon. CH_3F has two types of states, ortho and para,

*Email address: chapovsky@iae.nsk.su

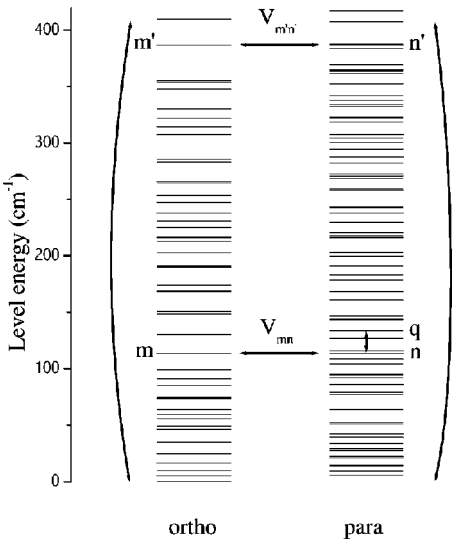

FIG. 1. Position of rotational levels of $^{13}CH_3F$. Molecular parameters are from Ref. [15]. Two pairs of states important for spin conversion in this molecule are indicated. The small vertical line in the para subspace indicates microwave excitation of the transition $n \rightarrow q$. Two bent vertical lines indicate rotational relaxation. Parameters of the important states are summarized in Table I.

shown in Fig. 1. The data in this figure correspond to the $^{13}CH_3F$ molecule and have been calculated using the molecular parameters from [15]. Spin isomers of CH_3F are distinguished by the total spin of the three hydrogen nuclei, $I=3/2$ for ortho and $I=1/2$ for para isomers. For ortho isomers only rotational quantum numbers $K=0,3,6,\ldots$ are allowed (K is the projection of molecular angular momentum **J** on the molecular symmetry axis.) For para molecules only $K=1,2,4,5,\ldots$ are allowed [1].

There are two close pairs of ortho and para states in the ground vibrational state of $^{13}CH_3F$ that are significantly mixed by the intramolecular perturbation $\hat{V}$ and that are important for the ortho-para conversion in the molecule. For a qualitative description, let us take into account only one of these pairs, $m-n$, and first assume that there is no external radiation. Suppose that the test molecule is placed into the ortho subspace. Due to the rotational relaxation caused by collisions, the molecule shuttles up and down along the ladder of rotational states. Nonmagnetic collisions do not change the nuclear-spin state directly, i.e., the relevant cross section is zero, $\sigma(\text{ortho}|\text{para})=0$. This shuttling along the rotational states inside the ortho subspace continues until the molecule jumps to the state m. During the free flight after that collision, the intramolecular perturbation $\hat{V}$ admixes the para states n to the ortho state m. Consequently, the next collision has a probability (usually very small) of transferring the molecule to other para states. This localizes the molecule inside the para subspace and the spin conversion occurs. This is the mechanism of radiation-free nuclear-spin conversion induced by the intramolecular state mixing [16] (see also Ref. [17]).

In the case of a strong microwave radiation applied to the molecular transition q-n in the para subspace, mixing of the states is affected by the radiation which allows one to control the ortho-para conversion. Influence of the radiation comes through three major effects: level shift (dynamical Stark effect, well known in nonlinear laser spectroscopy [18,19]), level population change, and light-induced coherence. In general, these three effects cannot be separated and these work together.

TABLE I. Positions of levels in $^{13}CH_3F$. Molecular parameters are from Ref. [15].

Notation	J,K	I	E (cm^{-1})	Frequency (MHz)
m'	20,3	3/2	387.1	351.01 ± 0.16 $(m'-n')$
n'	21,1	1/2	387.1	
q	12,1	1/2	133.7	596294.285 ± 0.013 $(q-n)$
n	11,1	1/2	113.8	130.99 ± 0.15 $(n-m)$
m	9,3	3/2	113.8	596425.28 ± 0.15 $(q-m)$

[a]Notation in Fig. 1.

In order to consider a real molecule, the above simplified picture has to be developed further. One has to account for the molecular center-of-mass motion. Although the intramolecular mixing does not depend on molecular velocity, the interaction of the molecule with the radiation does. Consequently, the ortho-para state mixing in coherent control also depends on molecular velocity.

Another complication comes from the degeneracy of molecular states. Even for the simplest case of pure polarization (linear or circular) of the radiation there are many excitation channels each having its own absorption coefficient and saturation parameter. These channels differ by the M-quantum number, the projection of **J** on the laboratory axis of quantization. It is important also to keep in mind that there are other degeneracies of states. Each state of $^{13}CH_3F$ in Fig. 1 is determined by the set of rotational quantum numbers (J,K,M), total spin of the three hydrogens, I, its projections on the laboratory z axis, σ, and z projections of the spins of the carbon and fluorine nuclei, both having spin $\frac{1}{2}$. The energy of rotational states of CH_3F depends only on J and K quantum numbers if tiny hyperfine contribution to the level energy is neglected. We conclude the qualitative picture by summarizing important parameters of $^{13}CH_3F$ in Table I.

A quantitative analysis of the isomer coherent control will be performed using the kinetic equation for the density matrix $\hat{\rho}$. The molecular Hamiltonian reads

$$\hat{H}=-(\hbar^2/2m_0)\nabla_{\mathbf{r}}^2+\hat{H}_0+\hbar\hat{G}+\hbar\hat{V}. \tag{1}$$

Here the first term is the Hamiltonian of the molecular center-of-mass motion; m_0 is the molecular mass. The main part of the molecular internal Hamiltonian, $\hat{H}_0$, has the ortho and para eigenstates shown in Fig. 1. $\hbar\hat{G}$ describes the molecular interactions with the external radiation that will be taken in the form of monochromatic traveling wave,

$$\hat{G}=-(\mathbf{E}\hat{\mathbf{d}}/\hbar)\cos(\omega_L t-\mathbf{k}\cdot\mathbf{r}), \tag{2}$$

where $\mathbf{E}$, ω_L, and $\mathbf{k}$ are the amplitude, frequency, and wave vector of the electromagnetic radiation, respectively; $\hat{\mathbf{d}}$ is the

operator of the molecular electric dipole moment. $\hat{V}$ is the intramolecular perturbation that mixes the ortho and para states in $^{13}CH_3F$. The spin-spin interaction between the molecular nuclei mixes the m-n pair ($J=9$, $K=3-11$, 1) [17,20]. The m'-n' pair (20,3–21,1) is mixed by the spin-spin and spin-rotation interactions [17,21–23]. Accounting for level degeneracy in light-molecule interactions is, in general, a difficult problem. The simplest case is that of a pure linear or circular polarization. We will consider electromagnetic radiation of linear polarization.

In the representation of the eigenstates of $\hat{H}_0$ (α states) and classical description of the molecular center-of-mass motion, the kinetic equation for the density matrix $\boldsymbol{\rho}$ reads [18]

$$\partial\boldsymbol{\rho}/\partial t+\mathbf{v}\cdot\boldsymbol{\nabla}\boldsymbol{\rho}=\mathbf{S}-i[\mathbf{G}+\mathbf{V},\boldsymbol{\rho}]. \tag{3}$$

Here $\mathbf{S}$ is the collision integral; $\mathbf{v}$ is the molecular center-of-mass velocity. Spontaneous decay is not included in this equation because it is negligible for rotational transitions in comparison with collisional relaxation.

A kinetic equation for the total concentration of para molecules can be obtained directly from Eq. (3),

$$\partial\rho_p/\partial t=-2\mathrm{Re}\int i\left(\sum\rho_{m'n'}V_{n'm'}+\sum\rho_{mn}V_{nm}\right)d\mathbf{v}. \tag{4}$$

Summation in the first and second terms is carried over all degenerate sublevels of the states m',n' and m,n, respectively. In Eq. (4) the total concentration of para molecules, $\rho_p=\Sigma_\alpha\int\rho_p(\alpha,\mathbf{v})d\mathbf{v}$, $\alpha\in$ para and a uniform spatial distribution of molecular density was assumed. Collision integral did not enter into Eq. (4) because by assumption collisions do not change the molecular spin state, i.e., $\Sigma_\alpha\int S_{\alpha\alpha}d\mathbf{v}=0$, if $\alpha\in$ ortho, or $\alpha\in$ para. $\mathbf{G}$ did not enter into Eq. (4) either because the matrix elements of $\mathbf{G}$ off-diagonal in nuclear-spin states vanish.

The off-diagonal matrix elements ρ_{mn} and $\rho_{m'n'}$ will be found in perturbation theory. Further we assume the perturbations $\hat{V}$ being small and consider zero- and first-order terms of the density matrix,

$$\boldsymbol{\rho}=\boldsymbol{\rho}^0+\boldsymbol{\rho}^1. \tag{5}$$

Collisions in our system will be described by a model that is standard in the theory of light-molecule interactions. The off-diagonal elements of $\mathbf{S}$ have decay terms only,

$$S_{\alpha\alpha'}=-\Gamma\rho_{\alpha\alpha'},\quad \alpha\neq\alpha'. \tag{6}$$

The decoherence rates Γ are taken to be equal for all off-diagonal elements of the collision integral. This assumption simplifies the theoretical model. Note that the dependence of the relaxation rates on rotational quantum numbers is known [24].

The diagonal elements of $\mathbf{S}$ are expressed through the kernel of the collision integral A in a usual way,

$$S(\alpha,\mathbf{v})=\sum_{\alpha_1}\int A(\alpha,\mathbf{v}|\alpha_1,\mathbf{v}_1)\rho(\alpha_1,\mathbf{v}_1)d\mathbf{v}_1 - \rho(\alpha,\mathbf{v})\sum_{\alpha_1}\int A(\alpha_1,\mathbf{v}_1|\alpha,\mathbf{v})d\mathbf{v}_1. \tag{7}$$

We consider the model of strong collisions with the following collision kernel for para molecules:

$$A(\alpha,\mathbf{v}|\alpha_1,\mathbf{v_1})=\nu_r w_p(\alpha)\delta(\mathbf{v}-\mathbf{v_1})+\nu_t\delta_{\alpha\alpha_1}f(\mathbf{v}),\quad \alpha,\alpha_1\in\text{para}, \tag{8}$$

and a similar equation for ortho molecules. $w_p(\alpha)$ in Eq. (8) is the Boltzmann distribution of rotational state populations of para molecules,

$$w_p(\alpha)=Z_p^{-1}\exp(-E_\alpha/k_BT), \tag{9}$$

with Z_p being the rotational partition function; E_α being the rotational energy of the α state; T being the gas temperature; k_B being the Boltzmann constant. The symmetry of CH_3F is such that the partition functions for ortho and para molecules are practically equal at room temperature. Partition functions account for all degeneracies of states (see Ref. [17] for more details); $f(\mathbf{v})$ in Eq. (8) is the Maxwell distribution,

$$f(\mathbf{v})=\pi^{-3/2}v_0^{-3}\exp(-\mathbf{v}^2/v_0^2);\quad v_0=\sqrt{2k_BT/m_0}. \tag{10}$$

In Eq. (8), two relaxation rates were introduced, rotational relaxation (ν_r) that does not affect molecular velocity and translational relaxation ν_t that equilibrates velocity but does not change the rotational state. Note that the rotational relaxation is accompanied in our model by the relaxation in M quantum numbers. Note also that the collisions in the model do not change the molecular-spin state. The introduction of different relaxation rates for different degrees of freedom makes the model of strong collisions more accurate and flexible. It allows one to adjust the model to particular experimental conditions. Because of its simplicity, the model of strong collisions is often used in laser physics and nonlinear spectroscopy, see, e.g., Refs. [18,25,26]. Numerical values for the collisional parameters Γ, ν_r, and ν_t will be determined later.

III. MICROWAVE ABSORPTION

For the zero-order term of the density matrix one has the following kinetic equation:

$$\partial\boldsymbol{\rho}^0/\partial t+\mathbf{v}\cdot\nabla\boldsymbol{\rho}^0=\mathbf{S}^0-i[\mathbf{G},\boldsymbol{\rho}^0]. \tag{11}$$

The electromagnetic field is chosen to be resonant to the rotational transition of para molecules. Consequently, ortho molecules remain at equilibrium in the zero-order perturbation theory. For the level populations of ortho molecules one has

$$\rho_o^0(\alpha,\mathbf{v})=(N-\rho_p^0)w_o(\alpha)f(\mathbf{v}), \tag{12}$$

where N is the total concentration of molecules.

Equations (6), (7), (8), and (11) allow one to deduce an equation for the stationary populations of para molecules,

$$(\nu_r+\nu_t)\rho_p^0(\alpha,\mathbf{v})=\nu_r w_p(\alpha)\rho_p^0(\mathbf{v})+\nu_t f(\mathbf{v})\rho_p^0(\alpha) + \rho_p^0 p[\delta_{\alpha q}-\delta_{\alpha n}], \tag{13}$$

where the excitation probability p is defined as

$$\rho_p^0 p=\frac{2\Gamma|G_{qn}|^2}{\Gamma^2+(\Omega-\mathbf{k}\cdot\mathbf{v})^2}[\rho_p^0(n,\mathbf{v})-\rho_p^0(q,\mathbf{v})]. \tag{14}$$

In Eq. (13) the notations were introduced,

$$\rho_p^0(\mathbf{v})=\sum_{\alpha\in para}\rho_p^0(\alpha,\mathbf{v}); \quad \rho_p^0(\alpha)=\int\rho_p^0(\alpha,\mathbf{v})d\mathbf{v}. \tag{15}$$

Equation (14) is written in the rotating wave approximation. Nonzero matrix elements of **G** (electric field has linear polarization along the z axis) are given by

$$G_{qn}=G(M)e^{i(\mathbf{k}\cdot\mathbf{r}-\Omega t)}, \quad G(M)\equiv E_{10}(\overline{d_{10}})_{qn}/2\hbar, \tag{16}$$

where $\Omega=\omega_L-\omega_{qn}$ is the radiation frequency detuning from the absorption line center, ω_{qn}; the bar over a symbol indicates a time-independent factor; E_{10} and d_{10} are spherical components of the electric field and electric dipole moment vectors, respectively [1]. The matrix element of $\hat{d}_{10}$ reads [1]

$$|(\overline{d_{10}})_{qn}|^2\equiv|d(M)|^2=(2J_q+1)(2J_n+1) \times\begin{pmatrix} J_q & 1 & J_n \\ -K & 0 & K\end{pmatrix}^2\begin{pmatrix} J_q & 1 & J_n \\ -M & 0 & M\end{pmatrix}^2 d^2 \ , \tag{17}$$

where (:::) stand for $3j$ symbols and d is the permanent electric dipole moment of CH_3F, $d=1.86$ D [27].

Solution of Eq. (13) presents no difficulty and can be written in the form

$$\rho_p^0(\alpha,\mathbf{v})=\rho_p^0 w_p(\alpha)f(\mathbf{v})+\rho_p^0[(\tau_2-\tau_1)p_1 f(\mathbf{v})+\tau_1 p] \times[\delta_{\alpha q}-\delta_{\alpha n}], \tag{18}$$

where the relaxation times are $\tau_1=(\nu_r+\nu_t)^{-1}$, $\tau_2=\nu_r^{-1}$, and $p_1=\int p d\mathbf{v}$. We have separated here the field-induced contributions nonequilibrium in α and $\mathbf{v}$ and nonequilibrium only in α. Solution (18) shows that radiation affects the population of only two states, q and n. This is the consequence of the accepted simple model of collisions.

The excitation probability can be found from Eqs. (14) and (18),

$$p_1=\frac{0.5\Delta w}{\tau_1(\kappa R)^{-1}+\tau_2-\tau_1},$$

$$p=\frac{\Gamma^2 f(\mathbf{v})}{\Gamma_B^2+(\Omega-\mathbf{k}\cdot\mathbf{v})^2}\frac{p_1}{R}, \tag{19}$$

where the difference of the Boltzmann factors is $\Delta w=w_p(n)-w_p(q)$; the saturation parameter κ and saturation intensity S_{sat} are

$$\kappa=\frac{S}{S_{sat}}, \quad S_{sat}=\frac{c\Gamma\hbar^2}{8\pi\tau_1|d(M)|^2}; \tag{20}$$

the homogeneous linewidth is $\Gamma_B=\Gamma\sqrt{1+\kappa}$, and

$$R=\int\frac{\Gamma^2 f(\mathbf{v})d\mathbf{v}}{\Gamma_B^2+(\Omega-\mathbf{k}\cdot\mathbf{v})^2}. \tag{21}$$

This integral can be expressed through the probability integral, but for numerical calculations performed in this paper it is easier to calculate it directly.

In a similar way, one can obtain from the kinetic equation (11) the off-diagonal density matrix element

$$\overline{\rho}_{qn}^0=-i\frac{\rho_p^0}{\overline{G}_{nq}}\frac{p}{2\Gamma}[\Gamma+i(\Omega-\mathbf{k}\cdot\mathbf{v})]. \tag{22}$$

We can now adjust the parameters of the collision kernel (8). Kinetic equation (11) describes a diffusion process with the diffusion coefficient, $D=v_0^2/2\nu_t$. The diffusion coefficient for CH_3F is $D\simeq 10^2$ cm^2/s at a pressure of 1 Torr. This determines the velocity equilibration rate, $\nu_t=4.4\times10^7$ s^{-1}/Torr.

Attenuation of the radiation is given by $\hbar\omega_L\rho_p\Sigma_M p_1$. Consequently, the absorption coefficient $\chi(\Omega)$ is determined by the expression

$$\chi(\Omega)=\hbar\omega_L\rho_p S^{-1}\sum_M p_1. \tag{23}$$

In the low-field limit ($\kappa\to0$) it is reduced to

$$\chi_{low}(\Omega)=\frac{\hbar\omega_L}{2\tau_1}\rho_p\Delta w R_{low}\sum_M S_{sat}^{-1}, \tag{24}$$

where $R_{low}=\lim_{S\to0}R$ is the Voigt profile of the absorption line. If $\Gamma\gg kv_0$ the absorption line is a Lorentzian of width Γ. Experimental data on $\chi(\Omega)$ for the rotational 11,1 $\to$12,1 transition can be used to determine the value of Γ. Equally, broadening of any other rotational transition can be used because in our collision model (6) one has the same Γ

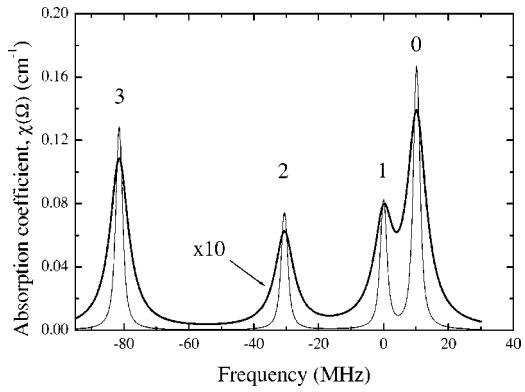

FIG. 2. Absorption spectrum near the 11,1→12,1 line. Numbers in the graph indicate the K values. The gas pressure is 30 mTorr. Low-intensity absorption is shown by the thin line, the case of $S=100$ mW/cm^2 is shown by the thick line.

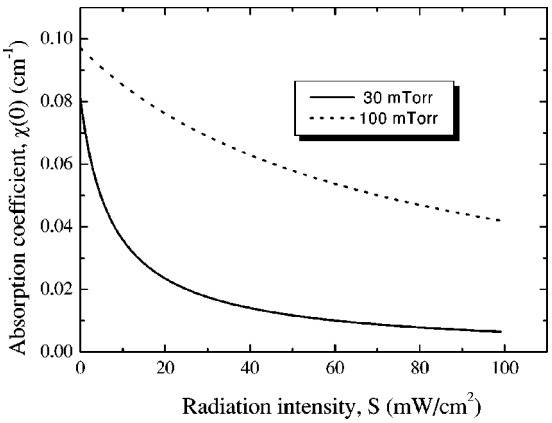

FIG. 3. Saturation of the absorption coefficient at the line center of the 11,1→12,1 transition. Gas temperature is $T=295$ K.

for all off-diagonal density-matrix elements. There are experimental results on broadening of the ortho-para (9,3)–(11,1) transition obtained from the level-crossing resonances in $^{13}CH_3F$ nuclear-spin conversion. This experiment gave the value $\Gamma/P=1.9\times10^8$ s^{-1}/Torr [28,29] that will be used in the present calculations. The last unknown parameter, rotational relaxation, ν_r, can be determined, e.g., from the power saturation of the absorption coefficient. This information is not available and we assume $\nu_r=\Gamma$. This is reasonable, because the pressure broadening in molecules is determined mainly by level population quenching, although this estimation for ν_r is probably too high.

We can now demonstrate the model at work by considering the microwave absorption by $^{13}CH_3F$. Absorption spectrum is determined by the selection rules $J\rightarrow J+1$, $K\rightarrow K$. The spectrum consists of groups of lines nearly equally separated by 50 GHz. Inside each group the lines, different in K, are rather dense. The spectrum near the 11,1→12,1 line is shown in Fig. 2. The two spectra correspond to low radiation intensity and to $S=100$ mW/cm^2 and the gas pressure equal to 30 mTorr in both cases.

Saturation intensity for the 11,1→12,1 line is equal to 43 W/cm^2 ($M=11$) and 6.8 W/cm^2 ($M=0$) at the gas pressure of 1 Torr. S_{sat} is proportional to the pressure squared, thus at 30 mTorr, $S_{sat}\simeq6$ mW/cm^2. An example of the absorption coefficient saturation is given in Fig. 3. Because the Doppler width of the transition is small, $kv_0=0.74$ MHz, low-field absorption at the line center depends weakly on CH_3F pressure if $P\gtrsim100$ mTorr. Another example of the saturation effect is shown in Fig. 4. Here the relative level population difference $[\rho_p(n)-\rho_p(q)]/\rho_p\Delta w$ is given as a function of radiation intensity. One can see that radiation having $S=100$ mW/cm^2 decreases the level population difference significantly.

IV. FIRST-ORDER THEORY

The kinetic equation for the first-order term of the density matrix $\boldsymbol{\rho}^1$ is obtained from Eq. (3),

$$\partial\boldsymbol{\rho}^1/\partial t+\mathbf{v}\cdot\nabla\boldsymbol{\rho}^1=\mathbf{S}^1-i[\mathbf{G},\boldsymbol{\rho}^1]-i[\mathbf{V},\boldsymbol{\rho}^0]. \tag{25}$$

Ortho-para conversion is determined by the terms $\rho^1_{m'n'}$ and ρ^1_{mn} because zero-order matrix elements off-diagonal in nuclear-spins vanish [see Eq. (4)]. Radiation does not affect the levels m' and n'. Consequently, the matrix element $\rho^1_{m'n'}$ is not different from the case of the field-free conversion [17],

$$\rho^1_{m'n'}=\frac{-iV_{m'n'}}{\Gamma+i\omega'}[\rho^0_p(n',\mathbf{v})-\rho^0_o(m',\mathbf{v})], \tag{26}$$

where $\omega'\equiv\omega_{m'n'}$. The density-matrix element ρ^1_{mn} can be obtained from the equations that are deduced from Eq. (25),

$$(\partial/\partial t+\mathbf{v}\cdot\boldsymbol{\nabla}+\Gamma)\rho^1_{mn}-i\rho^1_{mq}G_{qn}=-iV_{mn}[\rho^0_p(n,\mathbf{v})-\rho^0_o(m,\mathbf{v})],$$

$$(\partial/\partial t+\mathbf{v}\cdot\boldsymbol{\nabla}+\Gamma)\rho^1_{mq}-i\rho^1_{mn}G_{nq}=-iV_{mn}\rho^0_{nq}. \tag{27}$$

Substitutions, $V_{mn}=\overline{V}_{mn}e^{i\omega t}$, $(\omega\equiv\omega_{mn})$; $\rho^1_{mn}=\overline{\rho}^1_{mn}e^{i\omega t}$; $\rho^1_{mq}=\overline{\rho}^1_{mq}e^{i[(\Omega+\omega)t-\mathbf{k}\cdot\mathbf{r}]}$, transform Eqs. (27) to algebraic equations that can be easily solved. The density-matrix element that one needs for the kinetic equation (4) reads

$$\overline{\rho}^1_{mn}=-i\overline{V}_{mn}\frac{[\Gamma+i(\Omega+\omega-\mathbf{k}\cdot\mathbf{v})][\rho^0_p(n,\mathbf{v})-\rho^0_o(m,\mathbf{v})]+i\overline{G}_{qn}\overline{\rho}^0_{nq}}{(\Gamma+i\omega)[\Gamma+i(\Omega+\omega-\mathbf{k}\cdot\mathbf{v})]+|G(M)|^2}. \tag{28}$$

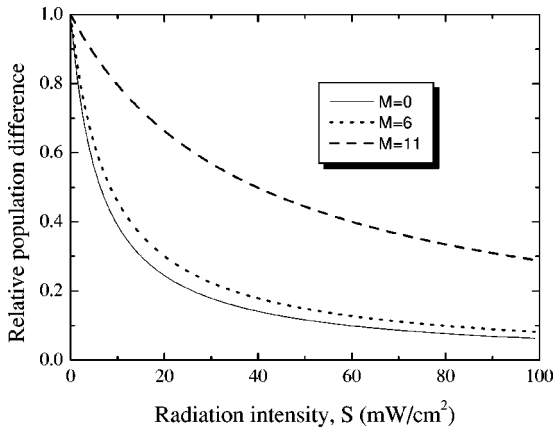

FIG. 4. Saturation of the level population difference normalized to the field-free population difference. The 11,1→12,1 transition. Gas pressure, $P=30$ mTorr; gas temperature, $T=295$ K.

Note that the indices m,n,q in Eqs. (28) represent the set of quantum numbers that describe all degenerate sublevels. Consequently, one has nonzero terms $\overline{\rho}^1_{mn}$ for the combination of quantum numbers that are allowed by the selection rules for $\hat{V}$.

V. CONVERSION RATES

Solutions for $\overline{\rho}^1_{m'n'}$ and $\overline{\rho}^1_{mn}$ together with the level populations from Eq. (18) and the off-diagonal matrix element from Eq. (22) allow one to present Eq. (4) as

$$\partial\rho_p/\partial t = N(\gamma'_{po}+\gamma_{po})-\rho_p\gamma,$$

$$\gamma \equiv \gamma'_{po}+\gamma'_{op}+\gamma_{po}+\gamma_{op}-\gamma_n-\gamma_c. \tag{29}$$

In this equation we have neglected the small difference between the total concentration of para molecules ρ_p, and its zero-order approximation ρ^0_p. The partial conversion rates in Eq. (29) have the following definition. The field-free conversion rate through the upper level pair, $m'-n'$,

$$\gamma'_{po} = \sum \frac{2\Gamma|V_{m'n'}|^2}{\Gamma^2+\omega'^2} w_o(m'). \tag{30}$$

Equation for γ'_{op} is obtained from γ'_{po} by substitution of the Boltzmann factor $w_p(n')$ instead of $w_o(m')$. Summation is made here over all degenerate substates of the m' and n' states. The rate γ_{po} is given by

$$\gamma_{po} = \sum |V_{mn}|^2 \left[\frac{2\Gamma}{\Gamma^2+\omega^2} + \mathrm{Re}\int F_1 f(\mathbf{v}) d\mathbf{v} \right] w_o(m). \tag{31}$$

An equation for γ_{op} is obtained from that for γ_{po} by substitution the Boltzmann factor $w_p(n)$ instead of $w_o(m)$. The rates γ_{po} and γ_{op} are field dependent. Their zero-field limits coincide with the field-free conversion rates through the pair of states $m-n$. The ''noncoherent'' contribution to the conversion, the rate γ_n, originating from the radiation-induced level population change in Eq. (28), is given by

$$\gamma_n = \sum |V_{mn}|^2 \left[\frac{2\Gamma\tau_2 p_1}{\Gamma^2+\omega^2} + 2\,\mathrm{Re}\int [(\tau_2-\tau_1)p_1 f(\mathbf{v}) + \tau_1 p] F_1 d\mathbf{v} \right]. \tag{32}$$

Finally, the ''coherent'' contribution to the conversion rate, γ_c, originating from the $\overline{\rho}^0_{nq}$ in Eq. (28), is

$$\gamma_c = \sum |V_{mn}|^2 \left[-\frac{p_1}{\Gamma^2+\omega^2} + \frac{1}{\Gamma}\mathrm{Re}\int p F_2 d\mathbf{v} \right]. \tag{33}$$

In Eqs. (31), (32), and (33) the following functions were introduced:

$$F_1 = \left(1-\frac{\Gamma_1+i\omega_1}{\Gamma+i\omega}\right)\frac{1}{\Gamma_1+i(\Omega+\omega_1-\mathbf{k}\cdot\mathbf{v})},$$

$$\Gamma_1 = \Gamma\left(1+\frac{|G(M)|^2}{\Gamma^2+\omega^2}\right),$$

$$F_2 = \frac{\Gamma+\Gamma_1+i\omega_1}{\Gamma+i\omega}\,\frac{1}{\Gamma_1+i(\Omega+\omega_1-\mathbf{k}\cdot\mathbf{v})},$$

$$\omega_1 = \omega\left(1-\frac{|G(M)|^2}{\Gamma^2+\omega^2}\right). \tag{34}$$

The introduced conversion rates can be interpreted as follows. Strong resonant radiation splits molecular states, changes level populations, and introduces coherences in the molecule. The field-dependent part of γ_{po} can be considered as being due to the radiation-induced level crossing. This term has resonance at $\Omega=-\omega_1$. The first term of γ_n is due to the population effect. It has the resonance at $\Omega=0$ where the excitation probability has maximum. The second part of γ_n is due to the population change and level crossing. It has two resonances, at $\Omega=0$ and at $\Omega=-\omega_1$. The coherent contribution γ_c also has resonances at these two frequencies.

The two peaks in the conversion rate spectra have rather distinctive features. The first one, at $\Omega=0$, is quite similar to the radiation-free conversion rate, e.g., γ'_{po} [Eq. (30)]. In our case $\omega\gg\Gamma$ and the amplitudes of the peaks at $\Omega=0$ are proportional to Γ, and thus to the gas pressure. In the limit $\omega\gg\Gamma$, contributions to the conversion rate provided by these terms are similar to the ordinary gas-kinetic processes that are proportional to the gas pressure also.

The resonances at $\Omega=-\omega_1$ have a completely different signature that would result from a field free conversion pattern of a degenerate ortho-para level pair. In this case the conversion rate has $1/\Gamma$ dependence, see, e.g., Eq. (30). It allows us to refer to the resonances at $\Omega=-\omega_1$ as produced by the crossing of the ortho and para levels and resulting

from the applied electromagnetic field. To reveal this property of the resonances at $\Omega=-\omega_1$, let us estimate the integral,

$$I=\int \frac{f(\mathbf{v})d\mathbf{v}\cdot}{\Gamma_1+i(\Omega+\omega_1-\mathbf{k}\cdot\mathbf{v})}, \tag{35}$$

at the radiation frequency $\Omega=-\omega_1$. In the limit of large Doppler broadening, $\Gamma_1 \ll kv_0$, the integrand in Eq. (35) has sharp resonance at $\mathbf{v}=\mathbf{0}$. One can substitute $f(\mathbf{v})$ by $f(0)$ in Eq. (35) and obtain $I\propto 1/kv_0$. Thus, the conversion is produced through the degenerate ortho-para level pair (level crossing) having the width equal to the Doppler width, kv_0. In the opposite limit of large homogeneous broadening, $\Gamma_1 \gg kv_0$, one can neglect $\mathbf{k}\cdot\mathbf{v}$ in the denominator of the integrand (35) and obtain $I\propto 1/\Gamma_1$. Again, this is the conversion through the crossed ortho and para states but now having the width Γ_1.

It would be useful to compare the results of the present model with the qualitative model [10]. This comparison cannot be made directly because in Ref. [10] rovibrational excitation of CH_3F was considered. But one can apply the idea of light-induced enrichment solely through the level population change and make the comparison. In the present notations, the field effect from the level population change is given by the first term in Eq. (32),

$$\gamma_{n1}=\sum \frac{2\Gamma|V_{mn}|^2}{\Gamma^2+\omega^2}\tau_2 p_1. \tag{36}$$

It gives a larger amplitude for the peak at $\Omega=0$ than the present model. In the present model one has partial cancellation of peaks at $\Omega=0$, see the first terms in the expressions for γ_n and γ_c. Because of the assumption, $\Gamma=\nu_r$, made in the collision model we have two times smaller peak at $\Omega=0$ in the present model. The cancellation is less significant if Γ is larger in comparison with ν_r.

We turn now to numerical calculations of the conversion rates in $^{13}CH_3F$. Contribution from the $m'-n'$ pair is difficult to calculate using Eq. (30) directly because of some uncertainty in the parameters involved. Instead, one can use the experimental value, $\gamma'_{po}=2.3\times10^{-3}$ s^{-1}/Torr [28,29] and scale it linearly in pressure. Such pressure dependence for γ'_{po} is valid if $\Gamma \ll \omega'$ [see Eq. (30)] which is fulfilled for the pressures $P<10$ Torr.

Calculation of the rates γ_{po}, γ_n, and γ_c requires the matrix elements V_{mn}. Mixing of the states m and n is performed by the intramolecular spin-spin interaction between the nuclei of $^{13}CH_3F$. Dependence of V_{mn} on nuclear-spin variables is easily accounted for by summation because other factors in Eqs. (31)–(33) do not depend on nuclear-spins. Then, the only remaining degeneracy is in the M-quantum numbers. This quantity reads

$$\sum |V_{mn}|^2=(2J_m+1)(2J_n+1)\begin{pmatrix} J_m & 2 & J_n \\ -K_m & q & K_n \end{pmatrix}^2 \times\begin{pmatrix} J_m & 2 & J_n \\ -M' & M'-M & M \end{pmatrix}^2 \mathcal{T}^2_{2,q}. \tag{37}$$

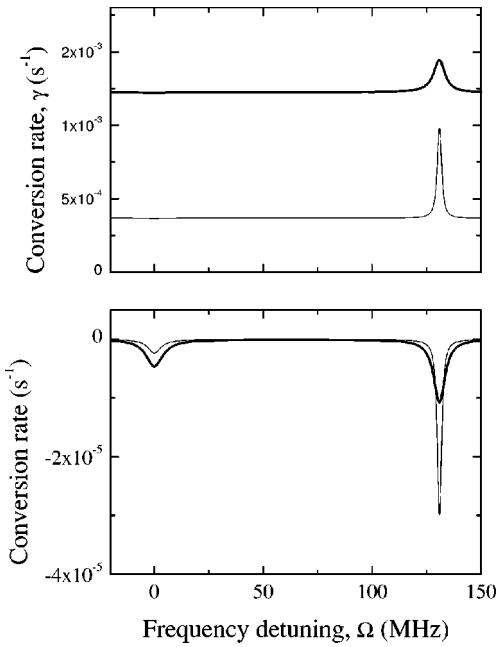

FIG. 5. Conversion rates. The upper panel shows the total conversion rate γ for the pressures $P=30$ mTorr (thin line) and $P=100$ mTorr (thick line). The lower panel shows the field-dependent contribution $-(\gamma_n+\gamma_c)$ at the pressures $P=30$ mTorr (thin line) and $P=100$ mTorr (thick line). The radiation intensity is $S=100$ mW/cm^2.

Here $\mathcal{T}_{2,q}$ $(q=K_m-K_n=2)$ is the magnitude of the spin-spin interaction and summation is carried over all nuclear-spin projections. The value of $\mathcal{T}_{2,2}$ calculated from the molecular structure is equal to 69.2 kHz. This value is confirmed by the experiment [30]. But in this paper we have to take a somewhat smaller value, $\mathcal{T}_{2,2}=64.1$ kHz, as it was obtained self-consistently for the three parameters, $\mathcal{T}_{2,2}$, Γ, and γ'_{po} [29].

Examples of the conversion rates are shown in Fig. 5. The upper panel gives the rate γ for two pressures, 30 mTorr and 100 mTorr. The radiation intensity in both cases is equal to 100 mW/cm^2. One can see that the peak at $\Omega=-\omega_1$ is $\simeq 3$ times larger at 30 mTorr than at 100 mTorr. There is also peak at $\Omega=0$ having "negative amplitude" but it is too small to be visible in the upper panel. The lower panel shows the field-dependent rates, $-(\gamma_n+\gamma_c)$. They are taken with the same sign as they contribute to γ in Eq. (29). One can see from this panel that the pressure dependences of the amplitudes of these two peaks are opposite. This is the consequence of the crossing of ortho and para states at $\Omega=-\omega_1$ and the off-resonant nature of the peak at $\Omega=0$.

The broadening of the two peaks in the conversion rate is very different too. The peak at $\Omega=0$ has broadening similar to that of an ordinary absorption line. At large saturation parameter κ, its width is $\sim 2|G|$ and grows rather fast with intensity. The width of the peak at $\Omega=-\omega_1$ is given by $\simeq\Gamma(1+|G|^2/\omega^2)$. Consequently, the power broadening of this peak is very small at our conditions. Figure 5 illustrates the difference in the peak widths.

VI. ENRICHMENT

The solution of the kinetic equation (29) can be presented as

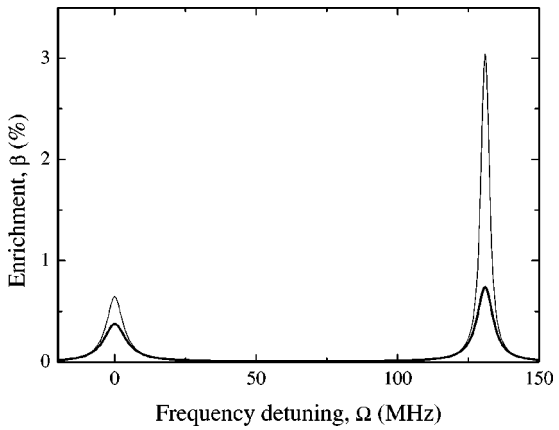

FIG. 6. Enrichment of para molecules β as a function of radiation frequency detuning Ω. Gas pressure $P=30$ mTorr (thin line); $P=100$ mTorr (thick line). In both cases the radiation intensity is $S=100$ mW/cm^2 and the gas temperature is $T=295$ K.

$$\rho_p(t)=\overline{\rho}_p+(\rho_p(0)-\overline{\rho}_p)\exp(-\gamma t),\quad \overline{\rho}_p=N(\gamma'_{po}+\gamma_{po})/\gamma, \tag{38}$$

where $\overline{\rho}_p$ and $\rho_p(0)$ are the steady-state and initial (equilibrium) concentrations of para molecules, respectively. Enrichment of para molecules will be defined as

$$\beta(\Omega)=\frac{\overline{\rho}_p}{\rho_p(0)}-1. \tag{39}$$

Partition functions for ortho and para isomers of CH_3F are equal. Consequently, $\gamma'_{po}=\gamma'_{op}$, $\gamma_{po}=\gamma_{op}$ and enrichment, $\beta(\Omega)$, can be expressed as

$$\beta(\Omega)=(\gamma_n+\gamma_c)/\gamma, \tag{40}$$

which will be used for the numerical calculations of $\beta(\Omega)$. One can note from Eq. (40) that despite the fact that the rates γ_{po} and γ_{op} have rather large field-dependent parts [see Fig. (5)], they alone would not produce an enrichment. It can be understood because these field-dependent parts are due to the mixing of states shifted by radiation but having equilibrium populations [see Eq. (31)]. Conversion through the mixing of equilibrium populated states does not affect the ortho-to-para ratio. Examples of the enrichment $\beta(\Omega)$ are given in Fig. 6. At the pressure 30 mTorr and radiation intensity $S=100$ mW/cm^2, the enrichment peak at $\Omega=-\omega_1$ is $\simeq 3\%$ and it is $\simeq 4$ times higher than the enrichment at $\Omega=0$. At larger radiation intensity, amplitude of the enrichment peak, $\beta(-\omega_1)$, saturates at $\simeq 5\%$. The peak at $\Omega=0$ grows to $\simeq 1\%$.

The simplified model that accounts only for the radiation-induced level population change predicts a factor of 2 higher peak at $\Omega=0$ than the present model. As was discussed above, in the present model one has partial cancellation of contributions originating from the rates γ_n and γ_c which results in a smaller enrichment. Another significant difference between these models is that the simplified model does not predict an enrichment at $\Omega=-\omega_1$.

Broadening of the two peaks in enrichment is very distinctive and is similar to the peaks of conversion rate, although there is some difference. The enrichment peak at $\Omega=-\omega_1$ is broader than the peak of γ because of large γ_{po} and γ_{op} at resonant frequency in the denominator of Eq. (40).

VII. DISCUSSION AND CONCLUSIONS

We have developed a model of spin-isomer coherent control that accounts for the molecular-level degeneracy in magnetic quantum numbers. This degeneracy together with the account of molecular center-of-mass motion allows one to apply the model to real molecules, having the actual level structure and ortho-para mixing Hamiltonian. The developed model was used to analyze the microwave induced enrichment of spin isomers in $^{13}CH_3F$. The conversion rate spectrum consists of two peaks with the peak at $\Omega=-\omega_1$ being two orders of magnitude higher than the peak at $\Omega=0$.

The enrichment spectrum also has two peaks at the same frequencies. One can obtain 3% enrichment using forbidden (for ordinary absorption) resonance at $\Omega=-\omega_1$, gas pressure 30 mTorr at room temperature, and radiation intensity $S=100$ mW/cm^2. The amplitude of the peak at $\Omega=0$ is four times smaller. Cooling the gas to 200 K would increase enrichment to $\simeq 5\%$ because of the increase of the level population difference. At higher radiation intensity enrichment saturates at $\simeq 5\%$ if the gas temperature is $T=295$ K and at $\simeq 7\%$ if $T=200$ K.

For the practical implementation of the microwave enrichment, the use of the peak at $\Omega=-\omega_1$ has several advantages. Enrichment here is significantly larger than at $\Omega=0$. Moreover, spurious effects can decrease the enrichment at $\Omega=0$ even further. This can be due to gas heating by radiation. Note that for the peak at $\Omega=-\omega_1$ absorption is negligible and there is no gas heating. Another spurious effect may be due to the resonant exchange of rotational quanta between ortho and para isomers. This effect prevents depopulation of one rotational state by radiation (state *n* in our case) in comparison with the population of the state *m* having nearly equal energy. Again, the peak at $\Omega=-\omega_1$ has the advantage of very low absorption coefficient and thus low radiation-induced population change. Finally, a disadvantage of the peak at $\Omega=0$ is the spurious absorption by the 11,0 $\rightarrow$12,0 line (Fig. 2). Although at low pressures this line is well separated from the 11,1$\rightarrow$12,1 line (the gap is 10 MHz), power broadening partially overlaps these lines. On the other hand, the $\Omega=-\omega_1$ peak is situated to the blue side of the 11,0$\rightarrow$12,0 line being 120 MHz away from the nearest absorption line (Fig. 2).

Enrichment obtained by microwave excitation of $^{13}CH_3F$ at reasonable experimental conditions is not large, $\simeq 3\%$. On the other hand, there are some applications where such enrichment could be significant, e.g., in spin-isomer-enhanced NMR techniques [8,7]. Note that for the standard 200 MHz NMR the difference in Boltzmann factors between Zeeman states, which determines the amplitude of the NMR signal, is only 3×10^{-5}. If even a fraction of the 3% isomer enrichment would be transferred to the Zeeman level populations it

would enhance the NMR signal significantly. To avoid any confusion we note that steady-state isomer enrichment requires that the microwave radiation be present permanently. If the radiation is turned off the enrichment decays with the radiation-free conversion rate.

Apart from any possible applications of microwave enrichment, which are presently too early to discuss, observation of the microwave enrichment would be important as a proof-of-principle demonstration of coherent control of spin isomers. It is interesting to note also that the isomer enrichment at $\Omega = -\omega_1$ would demonstrate an example of enhanced access to weak processes in molecules through isomer enrichment [31]. Suppose one would like to measure the absorption at $\Omega = -\omega_1$ directly. At the conditions considered in the paper, $\chi(-\omega_1) \simeq 6 \times 10^{-6}$ cm^{-1} which is rather difficult to measure. This value has to be compared with the 3% enrichment in the coherent control which should not be difficult to measure.

ACKNOWLEDGMENTS

The authors are indebted to K. A. Nasyrov for useful discussions of the light-molecule interaction theory and to D. Budker for a critical reading of the manuscript. This work was supported in part by the Russian Foundation for Basic Research (RFBR), Grant No. 01-03-32905.

[1] L.D. Landau and E.M. Lifshitz, *Quantum Mechanics*, 3rd ed. (Pergamon Press, Oxford, 1981).
[2] A. Farkas, *Orthohydrogen, Parahydrogen and Heavy Hydrogen* (Cambridge University Press, London, 1935), p. 215.
[3] E. Ilisca and S. Paris, Phys. Rev. Lett. **82**, 1788 (1999).
[4] E. Ilisca, Prog. Surf. Sci. **41**, 217 (1992).
[5] M. Quack, Mol. Phys. **34**, 477 (1977).
[6] D. Uy, M. Cordonnier, and T. Oka, Phys. Rev. Lett. **78**, 3844 (1997).
[7] J. Natterer and J. Bargon, Prog. Nucl. Magn. Reson. Spectrosc. **31**, 293 (1997).
[8] C.R. Bowers and D.P. Weitekamp, Phys. Rev. Lett. **57**, 2645 (1986).
[9] P.L. Chapovsky and L.J.F. Hermans, Annu. Rev. Phys. Chem. **50**, 315 (1999).
[10] L.V. Il'ichov, L.J.F. Hermans, A.M. Shalagin, and P.L. Chapovsky, Chem. Phys. Lett. **297**, 439 (1998).
[11] A.M. Shalagin and L.V. Il'ichov, Pis'ma Zh. Éksp. Teor. Fiz. **70**, 498 (1999) [JETP Lett. **70**, 508-513 (1999)].
[12] E. Ilisca and S. Sugano, Chem. Phys. Lett. **149**, 20 (1988).
[13] P.L. Chapovsky, Phys. Rev. A **63**, 063402 (2001).
[14] P.L. Chapovsky, M. Hepp, M.M. Beaky, I. Pak, and G. Winnewisser (private communication).
[15] D. Papoušek, J. Demaison, G. Wlodarczak, P. Pracna, S. Klee, and M. Winnewisser, J. Mol. Spectrosc. **164**, 351 (1994).
[16] R.F. Curl, Jr., J.V.V. Kasper, and K.S. Pitzer, J. Chem. Phys. **46**, 3220 (1967).
[17] P.L. Chapovsky, Phys. Rev. A **43**, 3624 (1991).
[18] S.G. Rautian, G.I. Smirnov, and A.M. Shalagin, *Nonlinear Resonances in Atom and Molecular Spectra* (Nauka, Novosibirsk, 1979).
[19] C. Cohen-Tannoudji, J. Dupont-Roc, and G. Grynberg, *Atom-Photon Interactions* (Wiley, New York, 1992).
[20] P.L. Chapovsky, J. Cosléou, F. Herlemont, M. Khelkhal, and J. Legrand, Eur. Phys. J. D **12**, 297 (2000).
[21] E. Ilisca and K. Bahloul, Phys. Rev. A **57**, 4296 (1998).
[22] K.I. Gus'kov, J. Phys. B: At. Mol. Opt. Phys. 32, 2963 (1999).
[23] P. Cacciani, J. Cosléou, F. Herlemont, M. Khelkhal, and J. Legrand, Eur. Phys. J. D **22**, 199 (2003).
[24] N.J. Trappeniers and E.W.A. Elenbaas-Bunschoten, J. Chem. Phys. **64**, 205 (1979).
[25] A.M. Dykhne and A.N. Starostin, Zh. Eksp. Teor. Fiz. **79**, 1211 (1980).
[26] V.R. Mironenko and A.M. Shalagin, Izv.Akad. Nauk SSSR, Seriya Fiz. **45**, 995 (1981) [Bull. Acad. Sci. USSR, Phys. Ser. (Engl. Transl.) **45**, 87 (1981)].
[27] S.M. Freund, G. Duxbury, M. Romheld, J.T. Tiedje, and T. Oka, J. Mol. Spectrosc. **52**, 38 (1974).
[28] B. Nagels, N. Calas, D.A. Roozemond, L.J.F. Hermans, and P.L. Chapovsky, Phys. Rev. Lett. **77**, 4732 (1996).
[29] P.L. Chapovsky, Appl. Magn. Reson. **18**, 363 (2000).
[30] J. Cosléou, F. Herlemont, M. Khelkhal, J. Legrand, and P.L. Chapovsky, Eur. Phys. J. D **10**, 99 (2000).
[31] P.L. Chapovsky, J. Phys. B: At. Mol. Opt. Phys. 34, 1123 (2001).